Top Catal (2011) 54:257–263
DOI 10.1007/s11244-011-9656-3

Improved Photocatalytic Degradation of Phenolic Compounds With ZnAl Mixed Oxides Obtained from LDH Materials

F. Tzompantzi · A. Mantilla · F. Bañuelos · J. L. Fernández · R. Gómez

Published online: 28 January 2011

Abstract ZnAl layered double hydroxides (LDHs) with different M_{II}/M_{III} molar ratio (0.89–3.81) were synthesized by the co-precipitation method and calcinated at 723 K. High specific surface areas (228–155 m^2/g) and semiconductor properties (band gap values from 3.32 to 3.07 eV) were obtained. The mixed oxides were reconstructed to the crystalline LDHs (memory effect) after being put in contact with aqueous solutions containing phenol and *p*-cresol. Using UV light, a maximum in photoactivity as a function of the Zn^{2+}/Al^{3+} molar ratio was observed. The sample with a Zn^{2+}/Al^{3+}molar ratio of 1.48 photodegrades up to 95% of phenol and *p*-cresol after 4 and 6 h of irradiation, respectively. These values are lower than that obtained with ZnO and commercial P-25 TiO_2 photocatalysts. The results show the applicability of alternative photocatalysts for the degradation of organic pollutant compounds rather than others such as TiO_2.

Keywords LDHs · Photocatalysts · Phenol photodegradation · *p*-cresol photodegradation · Zinc–aluminum mixed oxides

1 Introduction

Phenol and phenol derivates used as raw materials in petrochemical and chemical industries are considered one of the most common organic water pollutants because of its high toxicity, even at low concentrations. Several methods to remove phenol and its compounds from water have been reported in literature; they include biological, thermal and chemical treatments and the named advanced oxidation processes (AOPs) [1–4]. Photocatalytic purification of wastewater by irradiated semiconductor particles has proven to be very effective for AOP [1, 5, 6]. The photocatalytic process occurs as follows: when a semiconductor particle absorb a photon of energy equal to or greater than the band gap energy width, an electron is promoted from the valence band to the conduction band leaving behind an electron vacancy or hole in the valence band. The hole may react with surface-bound H_2O or HO^- producing the $OH^{\cdot}$ radicals, which are widely accepted to be the primary oxidizing species in the photocatalytic processes. The photocatalytic activity strongly depends on the energy of the electron–hole pairs produced as well as on their separation. A wider separation of the electrons and holes enhances the photocatalytic activity by reducing the electron–hole recombination [3]. The semiconductor materials most reported as photocatalysts are TiO_2, ZnO and SnO_2 [7–13]. However, some layered double hydroxides (or hydrotalcite type compounds) for example, ZnAl LDH have been recently reported as a good alternative for the photodegradation of pollutant organic compounds like methyl-orange [3], methylene blue [14] and phenol [15, 16] in aqueous media.

Layered double hydroxides (LDHs) are a family of lamellar solids which have received a considerable interest in recent years due to their potential application as basic catalysts [17], catalyst supports [18], adsorbents [19], anion exchangers [20], enzyme immobilizers [21] and medical oriented products [22], among others [23]. These applications are possible because of the possibility to obtain,

F. Tzompantzi · F. Bañuelos · R. Gómez
Departamento de química, Universidad Autónoma Metropolitana-Iztapalapa, Av San Rafael Atlixco No 186, México, DF 09340, Mexico
e-mail: fjtz@xanum.uam.mx

A. Mantilla (✉) · J. L. Fernández
CICATA-IPN, Av. Legaria No 694, México, DF 11500, Mexico
e-mail: angelesmantilla@yahoo.com.mx

throughout thermal decomposition of the layered precursor, mixed metal oxides at the atomic level, rather than at a particle level [3]. The general formula to describe the layered double hydroxides (LDHs) is: $[M^{2+}_{1-x}\ M^{3+}_{x}\ (OH)_2]^{x+}\ (A^{n-})_{x/n}$: y H_2O, where M^{2+} and M^{3+} are divalent and trivalent metal ions, respectively, and A^{n-} is an intercalate anion, being CO_3^{2-} the most common [18–20].

In the present work, the synthesis by the co-precipitation method of ZnAl LDHs with different Zn^{2+}/Al^{3+} molar ratio is reported. The objective is focused to demonstrate the importance of the Zn^{2+}/Al^{3+} molar ratio in the photoactivity. The characterization of the materials was made by means of X-ray diffraction (XRD), transmission electron microscopy (TEM), nitrogen adsorption and UV–vis spectroscopy. The photocatalytic behavior of calcinated and reconstructed LDHs materials was tested towards the decomposition of two important organic pollutants, phenol and *p*-cresol, in aqueous medium.

2 Experimental

2.1 Synthesis

ZnAl layered double hydroxides with different M^{2+}/M^{3+} ratio were prepared at constant pH by the co-precipitation method, using aqueous solutions of $Zn(NO_3)_2{\cdot}6H_2O$, and $Al(NO_3)_3{\cdot}9H_2O$ (J.T.Baker Analyzed Reagent). Both solutions were added dropwise in a stirring glass reactor containing 1000 mL of bidistilled water at 363 K; the pH of the solution was adjusted to nine by adding urea (NH_2CONH_2) as precipitant agent. The slurry was vigorously stirred for 4 h at 363 K and maintained under reflux for 36 h. Then, the resulting precipitate was filtered and washed with hot deionized water, dried at 373 K (dried samples) for 12 h and finally, annealed at 673 K for 12 h in air flow (2 mL/s) calcinated samples.

2.2 Characterization

XRD diffraction patterns of the dried solids were obtained with a Siemens D500 diffractometer ($\lambda = 0.1541$ Å). TEM micrographs were obtained with an electron microscope Carl Zeiss-EM910 with 120 kV and 0.6 nm of resolution. Before observation the samples were prepared using EPON 912 EMS. Cuts were made with an ultra-microtome RMC Mod MT 7000. BET specific surface areas were obtained on the calcinated samples from the nitrogen adsorption isotherms using a QUANTACHROME Autosorb-3B equipment. UV–vis absorption spectra for the different calcinated samples were obtained with a Cary-100 spectrophotometer and Eg was calculated from the value obtained by extrapolating the absorbance to the *x* axis curve for $y = 0$.

2.3 Photocatalytic Activity

The photodegradation of phenol and *p*-cresol in an aqueous medium using the calcinated samples as catalysts was carried out in a stirred Pyrex batch photoreactor; 200 mL of a solution containing 40 ppm (0.425 mmol) of phenol/g catalyst was irradiated with a UV Pen-Ray Power Supply (UVP Products 2.8 W, with $\lambda = 254$ nm and intensity of 4400 $\mu W/cm^2$), placed in a quartz tube, which was immersed in the solution. A series of reactors were put simultaneously with the solution containing the pollutant and the photocatalysts in dark for 1 h. After that, the UV lamp was turned "on" and aliquots were taken at different time intervals. The same procedure was followed to determine the photodegradation of *p*-cresol, but using a solution containing 80 ppm (0.738 mmol) of *p*-cresol/g catalyst. The pollutant concentration after irradiation was determined by UV–vis spectroscopy analysis following the 269 and 275 nm absorption bands for phenol and *p*-cresol, respectively.

The determination of total organic carbon was carried out as a function of time in the irradiated solution was carried out using a TOC-Vcpn analyzer Shimadzu. Also, in order to discard any confusion in the interpretation of the results due to the retention of reactants and intermediates on LDH, the powder was removed after the tests, dried and then, analyzed by FTIR in a Perkin-Elmer FT1730 spectrophotometer, using a nominal resolution of 4 cm^{-1} in order to improve the signal-to-noise ratio.

3 Results and Discussion

3.1 Molar Composition

Table 1 shows the molar composition measured by atomic absorption spectroscopy of LDHs dried at 373 K; the Zn^{2+}/Al^{3+} molar ratio of the samples were comprised between 0.89 and 3.81.

3.2 X ray Diffraction

XRD patterns of dried ZnAl LDHs are presented in Fig. 1. Hydrotalcite type structure was observed in all the samples.

Table 1 Zn^{2+}/Al^{3+} molar ratio for ZnAl LDH materials

Material	Name	Zn^{+2}/Al^{+3} molar ratio
$Zn_{0.89}$ Al	ZA1	0.89
$Zn_{1.07}$ Al	ZA2	1.07
$Zn_{1.47}$ Al	ZA3	1.47
$Zn_{1.67}$ Al	ZA4	1.67
$Zn_{3.81}$ Al	ZA5	3.81

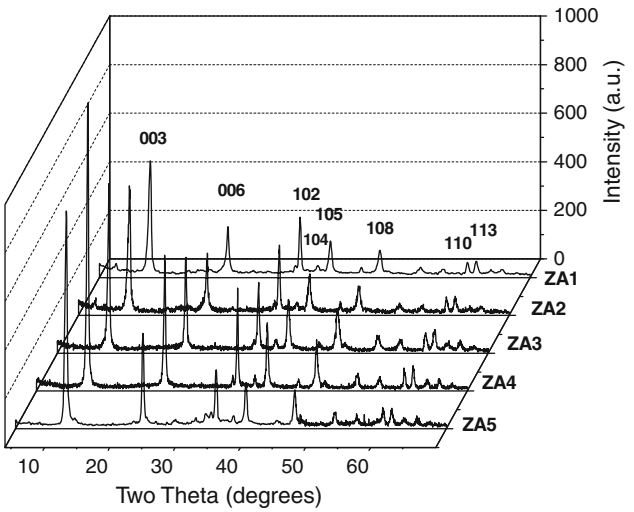

Fig. 1 X-ray diffraction patterns for ZnAl LDHs with different Zn^{2+}/Al^{3+} molar ratio

The 11.84 angle (003 planes) of two theta signal which corresponds to the interlamellar distance of the carbonated solid can be clearly seen. If an hexagonal packing is assumed, the cell parameter can be calculated by means of the 003 and 110 reflection values using the equations $c = 3d_{003}$ and $a = 2d_{110,}$ where c corresponds to three times the interlayer distance (003) and a is the average metal–metal distance in the interlayer structure (110).

The cell parameters show that the interlayer distance (d_{003}) was increased from 7.468 to 7.526 Å when the values of molar ratio Zn^{+2}/Al^{+3} were increased from 0.89 to 3.81 (Table 2). Seftel et al. [3] suggest that the variation in the cell parameter can due to the size, number, strength and orientation of the bonds between the anions and the hydroxyl groups in the LDH layer. Therefore, the increasing of the charge density could provoke the requirement of a higher amount of carbonate anions in order to maintain the electro-neutrality of the material.

3.3 Electron Microscopy

TEM image for the selected ZA3 LDH sample is presented in Fig. 2, where conglomerates lower than 100 nm can be seen. The characteristic lamellar structure of LDH can be clearly seen, confirming the crystalline structure observed by XRD.

Table 2 Cell parameters for Zn/Al LDHs materials

Catalyst	2θ (003)	2θ (110)	d_{003}	Parameter c (Å)	Parameter a (Å)
ZA1	11.84	60.38	7.468	22.405	3.063
ZA2	11.84	60.38	7.468	22.519	3.063
ZA3	11.84	60.41	7.468	22.405	3.062
ZA4	11.84	60.32	7.468	22.405	3.066
ZA5	11.75	60.23	7.525	22.576	3.070

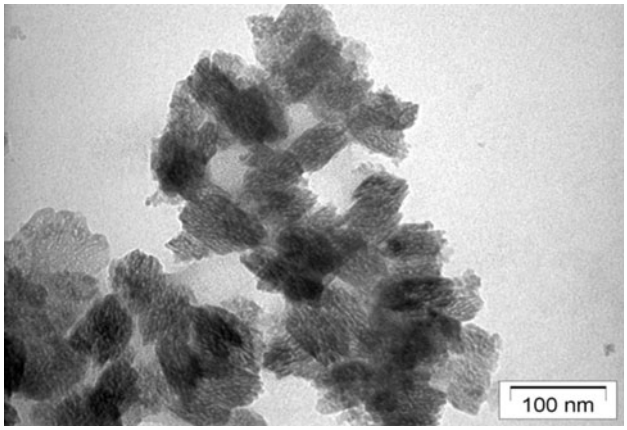

Fig. 2 TEM image of the ZA3 sample LDHs with a Zn^{2+}/Al^{3+} molar ratio of 1.47

3.4 Specific Surface Areas

The specific surface area values for the ZnAl mixed oxides at different Zn^{2+}/Al^{3+} molar ratio are reported in Table 3. A diminution in the specific surface area was observed for the samples with higher Zn^{2+}/Al^{3+} molar ratio. High specific surface areas in comparison to the values reported for ZnAl LDHs were obtained in all the samples and they are comprised between 228 and 155 m^2/g [24].

3.5 Band Gap Energy

The effect of the Zn^{2+} content in the bandgap (Eg) for the ZnAl oxides is shown in Fig. 3. The calculated Eg values were comprised between 3.07 and 3.32 eV. A minimum in the value of Eg as a function of the Zn^{2+}/Al^{3+} molar ratio was observed. The lowest energy value is that showed for the sample with a Zn^{2+}/Al^{3+} molar ratio of 1.47 (Table 3). The shift of the Eg band to higher energy around 3.3 eV may be due to Zn coordination with hydroxyl groups.

3.6 Phenol Photodegradation

Before the photodegradation tests, studies of adsorption and photolysis of the phenolic compounds on the annealed solids (673 K) were carried out putting in contact (in dark) 200 mL of the aqueous solutions of phenol and *p*-cresol with 0.2 g of calcined catalysts in a stirred Pyrex batch reactor during 1 h. No changes in the solution concentration measured by UV spectroscopy were observed.

After this period, the solids were recovered and analyzed by XRD in order to analyze the structural changes in

Table 3 Specific surface area, bandgap (Eg), first-order constant rate (K_{app}) and half-time ($t_{1/2}$) values for the photodegradación of phenol and *p*-cresol using TiO_2 commercial P-25, ZnO and reconstructed ZnAl mixed oxides with different Zn^{2+}/Al^{3+} molar ratio

Catalyst	Specific surface area (m^2/g)	Eg (eV)	Phenol (40 ppm)		*p*-cresol (80 ppm)	
			K_{app}	$t_{1/2}$ (h)	K_{app}	$t_{1/2}$ (h)
ZA1	228	3.14	0.093	7.5	0.261	2.6
ZA2	191	3.25	0.217	3.2	0.362	1.9
ZA3	169	3.07	0.989	0.7	0.457	1.5
ZA4	181	3.32	0.268	2.6	0.386	1.8
ZA5	155	3.20	0.157	4.4	0.061	11.3
TiO_2–P25	50	3.30	0.597	1.2	0.188	3.7
ZnO	55	3.01	–	–	0.051	13.5

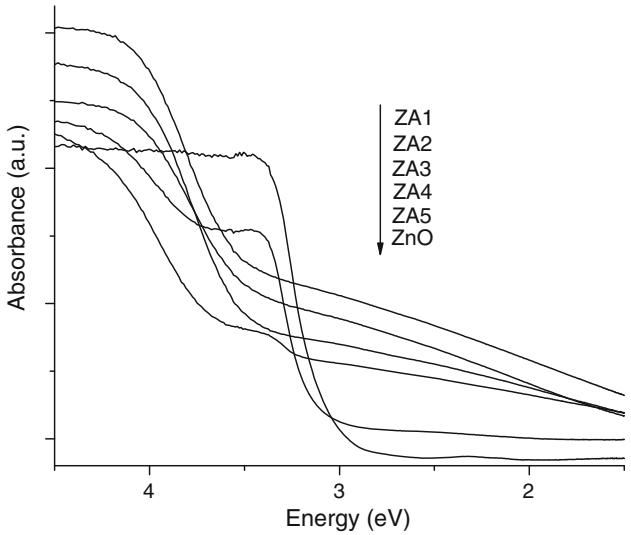

Fig. 3 UV–vis absorption spectra for calcinated materials with different Zn^{2+}/Al^{3+} molar ratio

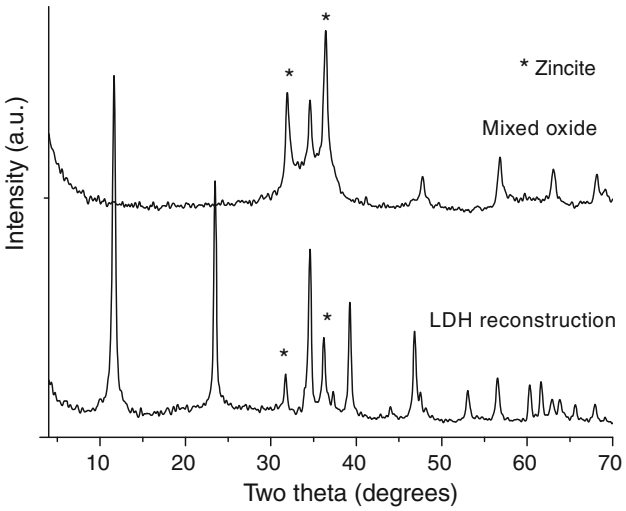

Fig. 4 XRD patterns for calcinated and reconstructed ZnAl LDH

the catalyst. The memory effect i.e. the reconstruction of the LDH structure was observed in all the samples; in Fig. 4, the XRD pattern of the AZ3 sample indicate a total destruction of the LDH crystalline structure on the calcinated sample; the presence of peaks denoting the formation of ZnO can be noted. However, the crystallinity of the LDH structure was recovered when the material was rehydrated and the presence of peaks identifying crystalline ZnO can be noted. Then, because of the fact of all the samples were put in contact with the pollutant solution before the photocatalytic test, we can consider that photodegradation was carried out with reconstructed LDHs solids.

Figure 5 shows the phenol photodegradation as a function of time using the various "in situ" reconstructed ZnAl LDHs. The best photodegradation result was reached with the ZA3 sample, which decomposes the phenol up to 95%, after 4 h of irradiation. The blank test (photolysis) showed that the UV lamp used in the present work is not capable to the phenol in the solution decompose by itself. There is an apparent small increase in the phenol concentration; this

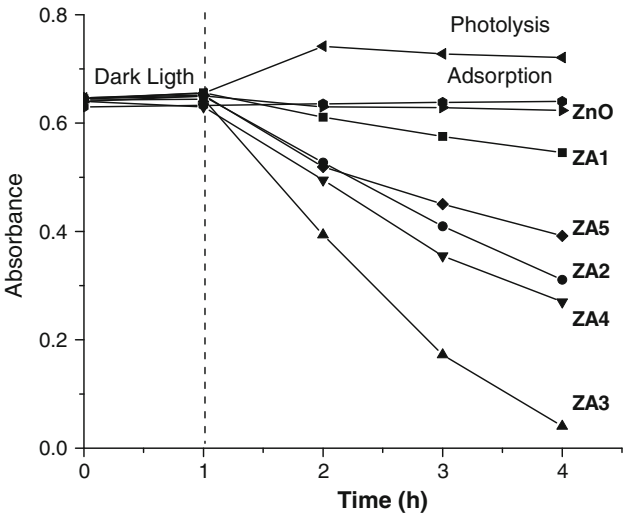

Fig. 5 Photodegradation of phenol (40 ppm) in aqueous solution on reconstructed ZnAl LDHs with different Zn^{2+}/Al^{3+} molar ratio

phenomenon may be due to some kind of modification suffered by the compound which increases the absorbance. Therefore, given this result, we can assume that phenol is

not photolyzed by UV light at 254 nm, and that any degradation observed is in fact due to the photocatalytic action of calcined LDHs.

The phenol photodegradation follows a pseudo first-order kinetic and the rate constant was evaluated from Fig. 6. In Table 3, the results of $t/_{1/2}$, which is the time required to decompose half of the phenol present in the irradiated solution were also included.

In order to show the applicability of ZnAl LDHs as photocatalysts, a comparative study of the behavior of TiO_2 commercial photocatalyst P-25 and ZnO for the photodegradation of phenol was included in this work and the results are shown in Table 3. The obtained values indicate that ZnAl LDHs are superior photocatalysts for the photodegradation of phenol; when ZnO was used as photocatalyst phenol was scarcely degraded.

3.7 *p*-Cresol Photodegradation

As for phenol, the study of photolysis produced in the solution containing 80 ppm of *p*-cresol (blank test) only irradiated with the UV lamps was made. It can be seen that the UV light source in absence of catalyst is not capable to degrade *p*-cresol.

The results of the photodegradation of *p*-cresol in aqueous solution (80 ppm) by using the ZnAl reconstructed mixed oxides and ZnO are presented in Fig. 7. It can be seen that the sample ZA3 (band gap 3.07) showed the highest photodegradation rate (up to 95%), after 5 h of irradiation. A pseudo first-order kinetic was found and the rate constant was evaluated from Fig. 8 and reported in Table 3. Although in this case it was a better photodegradation with ZnO, the results with all the ZnAl LDHs were superior.

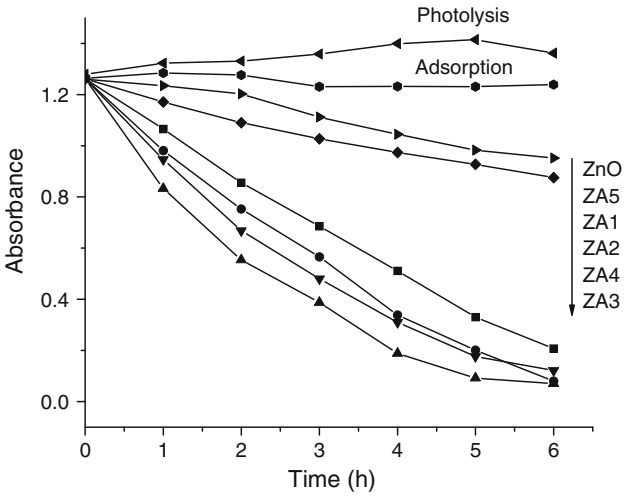

Fig. 7 Photodegradation of *p*-cresol (80 ppm) in aqueous solution on reconstructed ZnAl mixed oxides with different Zn^{2+}/Al^{3+} molar ratio

When photodegradation of organic compounds is carried out, it seeks to reach the total mineralization of the pollutants; however, the formation of some intermediates like hydroquinone or catechol has been reported for the phenolic compounds photo-oxidation [25]. Looking for the capacity of the LDH for a total mineralization of phenol and *p*-cresol, total organic carbon (TOC) analysis was carried out in the most active solids (ZA2, ZA3 and ZA4). The results obtained are reported in Figs. 9 and 10 for phenol and *p*-cresol respectively. It can be seen that, after 4 h of irradiation phenol was photodegraded up to 79, 88 and 95% for the ZA2, ZA4 and ZA3 LDHs respectively, while for the case of *p*-cresol photodegradation, it was mineralize up to 58, 67, and 78% after 6 h under irradiation

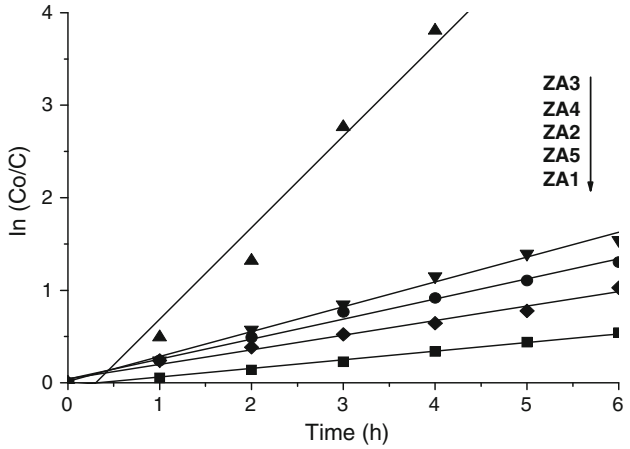

Fig. 6 Pseudo first-order kinetic for the photodegradation of phenol (40 ppm) on reconstructed ZnAl mixed oxides with different Zn^{2+}/Al^{3+} molar ratio

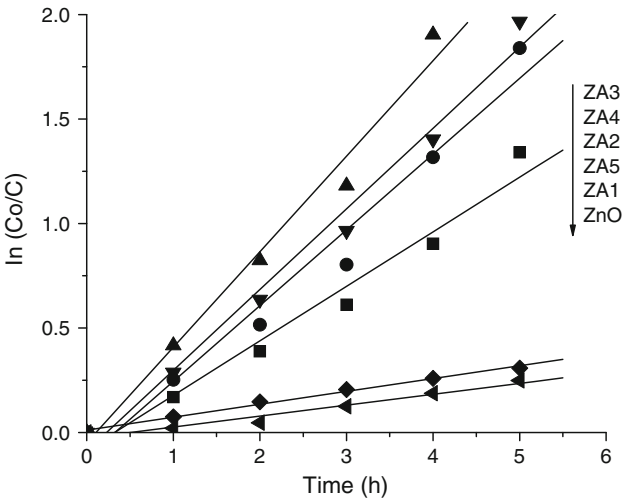

Fig. 8 Pseudo first-order kinetic for the photodegradation of *p*-cresol (80 ppm) using reconstructed ZnAl mixed oxides with different Zn^{2+}/Al^{3+} molar ratio

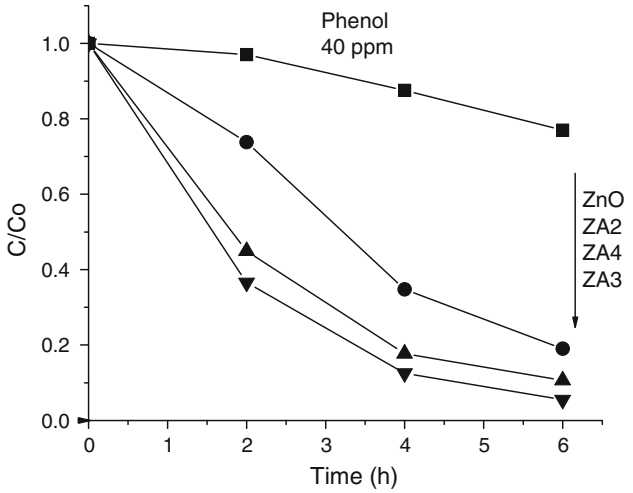

Fig. 9 TOC analysis for the photodegradation of 40 ppm of phenol with ZnO and ZnAl LDHs with different Zn^{2+}/Al^{3+} molar ratio

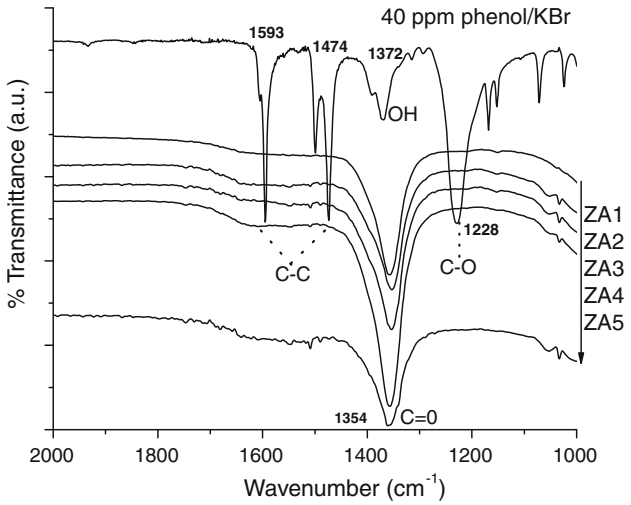

Fig. 11 FTIR analysis of ZnAl LDHs with different Zn^{2+}/Al^{3+} molar ratio after photodegradation of 40 ppm of phenol

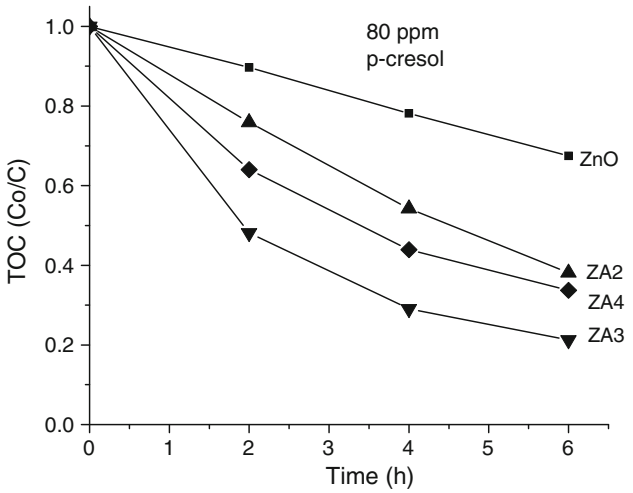

Fig. 10 TOC analysis for the photodegradation of 80 ppm of *p*-cresol with ZnO and ZnAl LDHs with different Zn^{2+}/Al^{3+} molar ratio

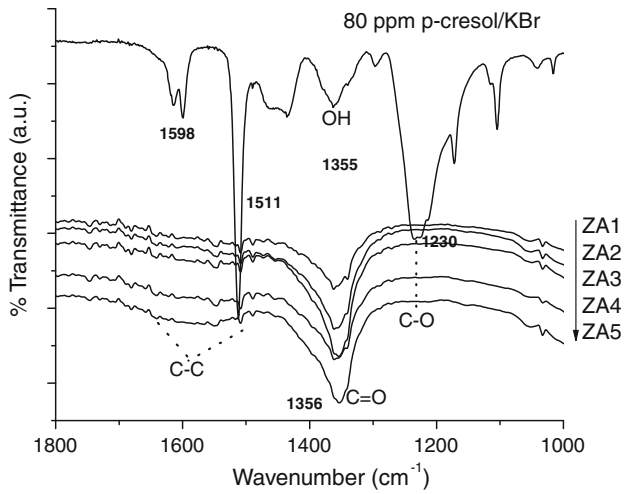

Fig. 12 FTIR analysis of ZnAl LDHs with different Zn^{2+}/Al^{3+} molar ratio after photodegradation of 80 ppm of *p*-cresol

in the presence of ZA2, ZA4 and ZA3 LDHs, respectively. These results showed that ZnAl LDHs are very efficient for the mineralization of phenolic compounds.

The results of the FTIR analysis of the recovery LDHs showed (Figs. 11, 12), that there are not peaks corresponding to phenol or *p*-cresol signal as well as their possible intermediates in the solids; the spectra correspond to carbonated LDHs. The characteristic band of the C–O-C bond at $\sim$1290 cm^{-1} can be seen in the spectra. Also, a strong band at 1320–1340 cm^{-1} indicates the presence of bidentate CO_3^{2-} anions in the interlayer region [26].

The effect of the Zn content on the ZnAl mixed oxides in the photodegradation of phenolic compounds can be explained according to the model showed in Fig. 13. The UV irradiation of the ZnAl mixed oxides provokes the

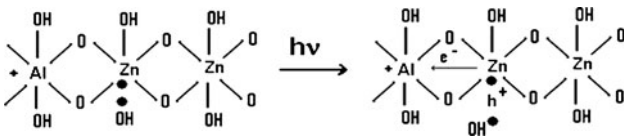

Fig. 13 Schematic representation for the generation of $OH^{\cdot}$ radicals in ZnAl LDHs

generation of electron–hole pairs, where the electron is delocalized towards the charge electro deficient Al^{3+}, generating the formation of the $OH^{\cdot}$ radicals which are the responsible of the photodegradation process [27].

In ZnAl mixed oxides, the Al^{3+} content plays an important role in the photodegradation process, since the positive charge of Al^{3+} favors the electron transfer generated during the formation of the $OH^{\cdot}$. The equilibrium

between the recombination rate and electron transfer will be more efficient to a given Zn^{2+}/Al^{3+} ratio. An excess of Zn^{+2} in the ZnAl LDHs does not favors the photo-efficiency [16]. Then, the presence of a maximum in the photodegradation of phenol and *p*-cresol as a function of the Zn^{2+}/Al^{3+} molar ratio can be expected. In the present study, the optimal Zn^{2+}/Al^{3+} molar ratio was 1.47 (ZA-3).

4 Conclusions

In this work it is showed that the ZnAl mixed oxides derived from the thermal decomposition of LDHs hydrotalcite type materials can be reconstructed "in situ". Good materials with improved photocatalytic properties for the photodegradation of phenol and *p*-cresol pollutants are then obtained from Zn/Al LDHs. It is proposed that the Zn^{2+} electron transfer to the Al^{3+} electro deficient cation produces a delay in the rate of the electron–hole pair recombination and hence an improvement of the photodegradation rate.

Acknowledgments We are indebted to SEP-CONACYT for the support provided to the CB-2006-1-62053 research project. A. Mantilla thanks CONACYT for scholarship support. We thank to Dr. Ulises Ruiz for the facilities of the chemistry laboratory of the Universidad Autónoma Metropolitana, Iztapalapa.

References

1. Busca G, Berardinelli S, Resini C, Arrighi L (2008) J Hazard Mater 160:265
2. Esplugas S, Gimenez J, Contreras S, Pascual E, Rodriguez M (2002) Water Res 36:1034
3. Seftel EM, Popovici E, Mertens M, De Witte K, Van Tendeloo G, Cool P, Vansant EF (2008) Microporous Mesoporous Mater 113:296
4. Andreozzi R, Caprio V, Insola A, Marotta R (1999) Catal Today 53:51
5. Rauf MA, Ashraf SS (2009) Chem Eng J. doi:10.1016/j.cej.2009.02.026
6. Vaccari A (1998) Catal Today 41:53
7. Lathasree S, Nageswara Rao A, SivaSankar B, Sadasivam V, Rengaraj K (2004) J Mol Catal A Chem 223:101
8. Saien J, Nejati H (2007) J Hazard Mater 148:491
9. Han F, Rao Kambala VS, Srinivasan M, Rajarathnam D, Ravi Naidu (2009) Appl Catal A Gen 359:25
10. Gaya UI, Abdullah AH, Photochem J, Photobiol C (2008) Photochem Rev 9:1
11. Pardeshi SK (2008) Sol Energy 82:700
12. Evgenidou E, Konstantinou I, Fytianos K, Poulios I, Albanis T (2007) Catal Today 124:156
13. Wang C, Xua B-Q, Wang X, Zhao J (2005) J Solid State Chem 178:3500
14. Parida M, Baliarsingh N, Sairam Patra B, Das J (2007) J Mol Catal A Chem 267:202
15. Kun R, Balázs M, Dékány I (2005) Colloid Surf A Physicochem Eng Aspects 265:155
16. Patzko A, Kun R, Hornok V, Dekany I, Engelhardt T, Schall N (2005) Colloid Surf A Physicochem Eng Aspects 265:64
17. Abelló S, Medina F, Tichit D, Pérez-Ramírez J, Sueiras JE, Salagre P, Cesteros Y (2007) Appl Catal B Environ 70:577
18. He FA, Zhang LM (2007) J Colloid Interf Sci 315:439
19. Cardoso LP, Valim JB (2006) J Phys Chem Solids 67:987
20. Goh H, Lima T-T, Dong Z (2008) Water Res 42:1343
21. Vial S, Prevot V, Leroux F, Forano C (2008) Microporous Mesoporous Mater 107:190
22. Xia S-J, Ni Z-M, Xu Q, Hu B-X, Hu J (2008) J Solid State Chem 181:2610
23. Melo F, Morlanés N (2008) Catal Today 133–135:374
24. Crespo I, Barriga C, Rives V, Ulibarri MA (1997) Solid State Ionics 101–103:729
25. Ortiz-Gomez A, Serrano-Rosales B, de Lasa H (2008) Chem Eng Sci 63:520
26. Di Cossimo JI, Díez VK, Xu M, Iglesia E, Apesteguía CR (1998) J Catal 178:499
27. Sauleda R, Brillas E (2001) Appl Catal B Environ 29:135